
000 UNDERSTANDING THE ROLE OF DEPTH IN THE NEU-
001 RAL TANGENT KERNEL FOR OVERPARAMETERIZED
002 NEURAL NETWORKS
003
004
005

006 **Anonymous authors**

007 Paper under double-blind review
008
009

010
011 ABSTRACT
012

013 Overparameterized fully-connected neural networks have been shown to
014 behave like kernel models when trained with gradient descent, under mild
015 conditions on the width, the learning rate, and the parameter initialization.
016 In the limit of infinitely large widths and small learning rate, the kernel that
017 is obtained allows to represent the output of the learned model with a closed-
018 form solution. This closed-form solution hinges on the invertibility of the
019 limiting kernel, a property that often holds on real-world datasets. In this
020 work, we analyze the sensitivity of large ReLU networks to increasing depths
021 by characterizing the corresponding limiting kernel. Our theoretical results
022 demonstrate that the normalized limiting kernel approaches the matrix
023 of ones. In contrast, they show the corresponding closed-form solution
024 approaches a fixed limit on the sphere. We empirically evaluate the order of
025 magnitude in network depth required to observe this convergent behavior,
026 and we describe the essential properties that enable the generalization of
027 our results to other kernels.

028 1 INTRODUCTION
029

030 Machine learning approaches have demonstrated a remarkable ability in helping solve a
031 multitude of problems across a large span of tasks. Whether the task is classification,
032 prediction, or image generation, some variants of the combination of a neural network plus
033 gradient descent have managed to achieve superhuman ability in some instances (LeCun
034 et al., 1998; Silver et al., 2018; Vaswani et al., 2017). In recent years, a particular observation
035 has been made regarding neural networks that are overparameterized. While previous
036 common thought indicated that these large networks would fall prey to overfitting, this
037 conclusion is being challenged empirically (Belkin, 2021). This phenomenon is not quite well
038 understood and it has led to works analyzing the learning dynamics of overparameterized
039 models updated with gradient descent (Liu et al., 2020; 2022; Jacot et al., 2018a). While
040 these works provide insight as to the learning dynamics of fully-connected neural networks
041 that are overparameterized, Jacot et al. (2018a), in particular, offer a closed-form solution
042 to the gradient flow based on a kernel that is recursively computed. This result offers the
043 possibility of approximately predicting the output of an overparameterized neural network
044 learned through gradient descent, without explicitly training the model. This comes at the
045 cost of computing a kernel over a particular dataset, which involves the computation of
046 expectations.

046 We focus on fully-connected ReLU networks, which allows us to both speed up the compu-
047 tation of the kernel and obtain a more interpretable closed-form solution. Leveraging this
048 more interpretable closed-form solution, we study the role of depth in the limiting kernel
049 of infinitely wide fully-connected ReLU networks. Our contributions address two central
050 aspects of the effect of increasing depths: 1) the convergence of the kernel, established in
051 Proposition 4, and 2) the limiting solution to the output of a fully-connected ReLU network
052 under infinitely wide hidden layers and infinitely small learning rate via Theorem 3. Our
053 results apply to arbitrary data with support on the sphere and, in contrast to previous
literature, do not require any assumptions on the spectrum of the Hermite expansion or

054 the Mercer decomposition of the kernel. The limiting solution we obtain does not require
055 any non-invertibility assumption as in [Xiao et al. \(2020\)](#) (see [Theorem 3](#) and the detailed
056 discussion following it). While the kernel of [Proposition 4](#) does converge to a constant matrix,
057 the limiting solution mentioned in 2) converges to a well-defined limit. We achieve this key
058 result by making use of rough differential equations machinery. In contrast to [Hanin & Nica
059 \(2020\)](#), we study the deterministic limit of the neural tangent kernel when the width is much
060 larger than the depth: while we allow the depth to increase to infinity, the rate at which it
061 does so is much slower than the widths of the hidden layers of a neural network. We offer a
062 summary of results in relation to ours in [table 1](#) in [Appendix E](#).

064 2 RELATED WORK

066 The learning dynamics of overparameterized neural networks have been extensively studied
067 through the lenses of kernel methods and Hessian-based analysis. A key development in
068 this area is the neural tangent kernel (NTK), introduced by [Jacot et al. \(2018a\)](#), which
069 describes how infinitely wide fully-connected neural networks trained with gradient descent
070 evolve linearly in function space. The NTK framework formalizes how, under common
071 assumptions—particularly Gaussian initialization and wide-layer limits—neural networks
072 behave similarly to kernel methods during training. [Arora et al. \(2019b\)](#) extend the NTK
073 to convolutional neural networks (CNN), further highlighting the framework’s capacity to
074 capture learning dynamics.

075 Subsequent work has reinforced the kernel-based interpretation of training dynamics through
076 analyses of the Hessian matrix. [Liu et al. \(2020; 2022\)](#) and [Belkin \(2021\)](#) demonstrate that
077 the loss landscape of overparameterized neural networks often exhibits near-linearity, with
078 low-curvature regions and small-norm Hessians, supporting the NTK-based approximation.
079 These findings suggest that network outputs are relatively stable during training, especially
080 for wide architectures with standard initialization. [Lee et al. \(2020\)](#) provide an in-depth
081 empirical analysis of NTK models and their performance compared to finite-width neural
082 networks of various architectures (e.g. fully-connected, CNNs). One key observation is that
083 NTKs often outperform finite-width networks, yet are usually surpassed by conventional
084 CNNs.

085 The NTK typically requires Monte Carlo estimation of expectations over Gaussian distribu-
086 tions, especially when nonlinearities from activations are involved. This reliance on sampling
087 can be computationally expensive and introduces variance in the resulting kernel evaluations.
088 However, closed-form expressions have been derived for certain activation functions, such as
089 ReLU and leaky ReLU ([Tsuchida et al. 2018](#)). Additionally, while prior work has largely
090 focused on width, less attention has been paid to how depth affects NTK sensitivity to
091 initialization and the associated multiplicity in network outputs. Among the few works
092 addressing this dimension, [Bietti & Bach \(2021\)](#) show that for the uniform measure on the
093 sphere, the reproducing kernel (c.f. reproducing kernel Hilbert space or RKHS) leads to the
094 same representation power regardless of the network depth. This raises the question of the
095 significance of depth for the NTK. [Lee et al. \(2022\)](#) present an analysis of deep narrow MLPs
096 and CNNs as depth goes to infinity. They provide a trainability guarantee, given the right
097 initialization, by showing convergence to a limiting kernel and a vanishing training error.
098 However, this initialization is not close to common initialization methods used in practice,
099 and it is still unclear whether deep narrow networks possess better generalization capabilities
100 than infinitely wide networks. Further insights are provided by [Nguyen et al. \(2021\)](#), who
101 derive an asymptotic lower bound on the smallest eigenvalue of the NTK through the Hermite
102 expansion of the kernel. This result can be used to derive bounds on the generalization of
103 the model ([Arora et al. 2019a](#)) and gives a better grasp on understanding the role that
104 depth plays in both convergence and generalization. [Murray et al. \(2023\)](#) characterize the
105 full spectrum of the NTK via the Hermite expansion for arbitrary datasets on the sphere.
106 They recover an empirical observation that the eigenvalues of the NTK follow power law
107 decay with respect to the size of the training set; [Li et al. \(2024\)](#) extend this line of results
to general domains beyond the sphere. In addition to the previous result from [Jacot et al.
\(2018a\)](#) regarding the convergence to kernel regression in the infinite width case, they also
establish a uniform convergence bound to the NTK regressor for the output of the trained

model. This improves upon the pointwise convergence bounds found in Lee et al. (2019); Arora et al. (2019b); Allen-Zhu et al. (2019). As in the initial paper by Jacot et al. (2018a), the limiting kernel is observed to be deterministic. This is contrasted with the work of Hanin & Nica (2020), where the authors characterize the NTK directly through the ratio of its second and first moment. They show that if the ratio of depth to width grows large, the NTK has a much higher variance than mean, implying that it is highly stochastic. Xiao et al. (2020) characterize three different phases describing the behaviour of the limiting kernel of infinitely wide neural networks. They show that the “ordered phase” and the “critical phase” can lead to generalization when trainable, while the “chaotic phase” collapses the mean-predictor to a (data-independent) constant predictor exponentially fast. Their proof in the ordered phase relies on the invertibility of a particular matrix and does not generalize to cases where this matrix is singular. This observation for the ordered phase has also been observed by Seleznova & Kutyniok (2022), who show that the NTK of infinitely large ReLU networks converges to a singular matrix. This reinforces the fact that small changes in the limiting kernels (as depth increases) can lead to significant changes in the mean-predictor.

3 NOTATION

To highlight the role of the depth L of a neural network, we denote elements that depend on layer $l \in \{1, \dots, L\}$ with a superscript (l) , e.g. $\kappa^{(l)}$. To emphasize the special role of the last layer in the analysis, the superscript (L) is sometimes used in mathematical objects to remind the reader of its link to a neural network of depth L , e.g. $\kappa^{(L)}$ refers to a network of depth L while it can also stand on its own as a mathematical object. The width of a layer l is denoted by n_l , with n_0 referring to the input dimension. Dependence on a time parameter t and the size n of a dataset is sometimes indicated with a subscript to emphasize their importance, but is otherwise omitted. A dataset of size n is denoted X , understood as an $n \times n_0$ matrix, where each row i is written as x_i^\top (i.e. the x_i 's are column vectors). It is assumed that all rows are different. Activation functions are denoted by σ , while uppercase Σ is reserved for computing “covariances” (see Definition 1). The limiting deterministic kernels of Jacot et al. (2018a) are represented using $\Theta_\infty^{(L)}$, and $\bar{\Theta}_\infty^{(L)}$ for their normalized version (see Definition 4); the notation κ is used when referring to general kernels and $\bar{\kappa}$ for the normalized version. For the sake of simplicity, we consider neural networks with one-dimensional outputs (i.e., $n_L = 1$). Therefore, kernels refer in this context to functions $\mathbb{R}^{n_0} \times \mathbb{R}^{n_0} \rightarrow \mathbb{R}_+$. We also write $\Theta(A)$ for the component-wise application of a kernel Θ to the entries of a matrix A . Specifically, $\kappa(XX^\top)$ denotes applying the kernel to all pairwise dot products in X , where XX^\top is the matrix containing those dot products. Similarly, for any function $g: \mathbb{R} \rightarrow \mathbb{R}$, the entry-wise application to a matrix A is denoted by $g(A)$. The notation $A \leftarrow_{i,j} A'$ refers to the matrix obtained by replacing column i of matrix A with column j of matrix A' . The vector of ones of length n is denoted $\mathbf{1}_n$. Finally, the sphere of dimension $n_0 - 1$ is denoted S^{n_0-1} .

4 BACKGROUND ON THE NTK AND OVERPARAMETERIZATION

Jacot et al. (2018a) show that, under overparameterization and i.i.d. standard normal weight initialization, a fully-connected neural network of arbitrary depth L exhibits learning dynamics that converge to those of kernel gradient flow in the infinite-width limit. They also provide a recursive formula to compute the kernel $\Theta_\infty^{(L)}$ to which gradient descent converges (see Theorems 1 and 2 from Jacot et al. (2018a)). However, evaluating $\Theta_\infty^{(L)}$ relies on computing high-dimensional expectations and can potentially also be subject to sample inefficiency in the approximation, motivating the search for a more readily computable kernel.

To make the kernel more practical, one may ask whether an efficient closed-form expression can be derived for particular activation functions. Of particular interest is the representation of $\Theta_\infty^{(L)}$ in closed-form when using ReLU activations (Tsuchida et al., 2018), due their empirical popularity and methodological appeal in theoretical analysis. In the rest of this paper, we will study this kernel for increasing L , with ReLU activation and $\mathcal{N}(0, 1)$ initialization. To

162 this end, let us first introduce important definitions and recap the recursive formulation of
 163 $\Theta_\infty^{(L)}$ by Jacot et al. (2018a).
 164

165 **Definition 1** ((mean) Covariance of neurons $\Sigma^{(l)}$). Let x and x' be two inputs in \mathbb{R}^{n_0} . The
 166 covariances of neurons from inputs x and x' at each layer l are defined recursively as

$$167 \Sigma^{(1)}(x, x') := \frac{1}{n_0} x^\top x', \quad \Sigma^{(l+1)}(x, x') := \mathbb{E}_{f \sim \mathcal{N}(0, \Sigma^{(l)})} [\sigma(f(x)) \sigma(f(x'))]$$

168 where $f \sim \mathcal{N}(0, \Sigma^{(l)})$ is an infinite vector indexed through the notation $f(x)$ and $f(x')$ and
 169 each vector $(f(x), f(x'))^\top \sim \mathcal{N}(0, \Sigma^{(l)}(x, x'))$. We also define the variant of $\Sigma^{(l)}$ where we
 170 replace σ with its derivative $\dot{\sigma}$:
 171

$$172 \dot{\Sigma}^{(l+1)}(x, x') := \mathbb{E}_{f \sim \mathcal{N}(0, \Sigma^{(l)})} [\dot{\sigma}(f(x)) \dot{\sigma}(f(x'))].$$

173 **Definition 2** (Neural tangent kernel (NTK)). For inputs x and x' , the neural tangent kernel
 174 of the neural network $f(\cdot; \theta)$ with parameters $\theta \in \mathbb{R}^P$ is given by

$$175 \Theta^{(L)}(x, x') = \sum_{p=1}^P \frac{\partial f(x; \theta_p)}{\partial \theta_p} \otimes \frac{\partial f(x'; \theta_p)}{\partial \theta_p}.$$

176 **Theorem 1** (Jacot et al. (2018a)). Suppose we have a fully-connected neural network of
 177 depth L with non-linear activation. In the limit as layer widths $n_1, \dots, n_{L-1} \rightarrow \infty$, the neural
 178 tangent kernel (see Definition 2) $\Theta^{(L)}$ converges in probability to a deterministic limiting
 179 kernel:
 180

$$181 \Theta^{(L)} \rightarrow \Theta_\infty^{(L)} \otimes I_{n_L},$$

182 where $\Theta_\infty^{(l)}$ is defined recursively by

$$183 \Theta_\infty^{(1)}(x, x') := \Sigma^{(1)}(x, x')$$

$$184 \Theta_\infty^{(l+1)}(x, x') := \dot{\Sigma}^{(l+1)}(x, x') \Theta_\infty^{(l)}(x, x') + \Sigma^{(l+1)}(x, x').$$

185 We remark that, although we assume $n_L = 1$ for the sake of simplicity, Theorem 1 is stated
 186 in its general form for any output dimension $n_L \in \mathbb{N}$. We also note that this is the version of
 187 the theorem without biases ($\beta = 0$ in the context of Jacot et al. (2018a)). This theorem is key
 188 in the convergence results obtained in the next section (Proposition 4 and Theorem 2). We
 189 are now ready to state the simplified formula for positively correlated inputs (Proposition 1).
 190

191 **Proposition 1.** For ReLU activation and perfectly positively correlated inputs x and x' , i.e.
 192 $\rho = 1$, it holds that

$$193 \Sigma^{(L)}(x, x') = \frac{1}{n_0 2^{L-1}} \|x\|_2 \|x'\|_2, \quad \dot{\Sigma}^{(L)}(x, x') = \frac{1}{2}$$

194 and

$$195 \Theta_\infty^{(L+1)}(x, x') = \frac{1}{2} \Theta_\infty^{(L)}(x, x') + \frac{1}{n_0 2^L} \|x\|_2 \|x'\|_2 = \frac{L+1}{n_0 2^L} \|x\|_2 \|x'\|_2.$$

196 *Proof sketch.* Note that $\frac{x^\top x'}{\|x\| \|x'\|} = 1$ and the product $\sigma^2(f(z))$, where $z \sim \mathcal{N}(0, 1)$, follows a
 197 squared rectified gaussian distribution, and that $\mu = 0$ implies $x^\top x' \geq 0$ with probability
 198 $\frac{1}{2}$. \square
 199

200 **Definition 3** (Correlation coefficient of $\Sigma^{(L)}(x, x')$). The correlations of neurons from inputs
 201 x and x' are defined as

$$202 \rho^{(L)}(x, x') := \frac{\Sigma^{(L)}(x, x')}{\sqrt{\Sigma^{(L)}(x, x) \Sigma^{(L)}(x', x')}}.$$

203 Note that $\rho^{(L)}(x, x') \in [-1, 1]$.
 204
 205

Proposition 2 (Arora et al. (2019b)¹). For datapoints x and x' with $\rho \in [-1, 1]$, it holds that

$$\begin{aligned}\rho^{(L+1)}(x, x') &= \frac{\sqrt{1 - (\rho^{(L)}(x, x'))^2}}{\pi} + \frac{\rho^{(L)}(x, x') \arcsin \rho^{(L)}(x, x')}{\pi} + \frac{1}{2} \rho^{(L)}(x, x') \\ \dot{\Sigma}^{(L+1)}(x, x') &= \frac{\arcsin \rho^{(L)}(x, x')}{2\pi} + \frac{1}{4}\end{aligned}$$

and

$$\Theta_{\infty}^{(L)}(x, x') = \|x\|_2 \|x'\|_2 \Theta_{\infty}^{(L)}\left(\frac{x}{\|x\|_2}, \frac{x'}{\|x'\|_2}\right)$$

for a fully-connected neural network with ReLU activation.

With these results, we achieved our goal of obtaining a closed-form expression for the $\Theta_{\infty}^{(L)}$ corresponding to an overparametrized (infinite-width), fully-connected ReLU network with no biases. This, in turn, allow us to aim at characterizing the output of such neural network, as done in the rest of the section. Indeed, from Proposition 2 and Proposition 2 from Jacot et al. (2018b), we can immediately observe a few facts regarding the input data:

- case a) If all datapoints lie on the unit sphere S^{n_0-1} , the NTK is invertible for $L \geq 2$ (Proposition 2 from Jacot et al. (2018b)).
- case b) If all datapoints are pairwise not colinear, i.e. $x_i^{\top} x_j < \|x_i\|_2 \|x_j\|_2$ for $i \neq j$, then the NTK is invertible (for $L \geq 2$) since we can project them to different points on the sphere through the canonical projection.
- case c) If we map points from \mathbb{R}^{n_0} to the sphere S^{n_0} by embedding them in a space of dimension $n_0 + 1$ and projecting them with the inverse stereographic projection (see Definition 7), the embedding of the datapoints satisfies $x_i^{\top} x_j = 1$ for all x_i, x_j in the dataset.

If one of these cases holds, the following proposition provides a closed-form expression for the approximation of the output of a fully-connected neural network.

Proposition 3 (Jacot et al. (2018a)). Let X be a dataset of size n (with entries x_i^{\top}) and let f^* and f_0 respectively refer to the learned function and the neural network after the initialization. If the limiting kernel $\kappa = \Theta_{\infty}^{(L)}(XX^{\top})$ is invertible, the output of the neural network converges to

$$f_{\infty}(x) = f_0(x) + \kappa_x^{\top} \kappa^{-1}(y^* - y_0),$$

where

$$\kappa_x = \Theta_{\infty}^{(L)}(xX^{\top}), \quad (y^*)_i = f^*(x_i), \quad (y_0)_i = f_0(x_i), \quad i = 1, \dots, n$$

as time $t \rightarrow \infty$, i.e. the number of gradient descent updates increases.

Motivated by Proposition 3 and the requirement to have an invertible κ , we identify **two** regimes of generalization: datapoints can lie on either a **1**) non-compact manifold (i.e. \mathbb{R}^{n_0}) or **2**) a compact manifold (i.e. S^{n_0-1}). The compact regime results in a simplifying assumption for the analysis that follows in this section. Note that one can project any dataset without any pair of colinear datapoints in \mathbb{R}^{n_0} on S^{n_0-1} using the canonical projection. The kernel κ will thus be invertible. If colinear points exist, an inverse stereographic projection embedding on S^{n_0} will result in an invertible κ .²

5 LIMITING KERNEL AS DEPTH INCREASES

While in the previous section, the depth L is fixed and the width goes to infinity, no mention is made of the effect of increasing both the depth and the width. Such insights into the

¹See also Cho & Saul (2009) for the complete derivation.

²In the context of learning the parameters of a neural network, we assume that one first projects onto the sphere and then fixes the projected data during the training phase.

270 additional effect of depth would provide a tangible frontier for the representation power of
 271 fully-connected neural networks and their generalization capabilities. In this section, we
 272 describe how the term κ_x from Proposition 3 approaches a fixed limit for each x as $L \rightarrow \infty$.
 273 The NTK will also approach this limit when $L \rightarrow \infty$, with $L \in o(\min_{l=1, \dots, L-1} n_l)$. Note
 274 that this setting is different from Hanin & Nica (2020), where the ratio of depth to width
 275 can be arbitrary; interestingly, when the depth grows faster than the width, there is no
 276 convergence to a deterministic limit for the NTK and it is stochastic. In this section, we
 277 always assume ReLU activation for $\Theta_\infty^{(L)}$ and $\Sigma^{(L)}$. For a concise list that summarizes the
 278 assumptions made in this section, we refer the reader to Appendix A.

279 The following lemma demonstrates that ρ converges to 1 for each pair of datapoints as L
 280 goes to infinity. This result is a key ingredient in the propositions and theorems that follow.

281 **Lemma 1** (Convergence of $\rho^{(L)}$). *If $\rho^{(1)}(x, x') \in]-1, 1[$, then $\rho^{(L)}(x, x') \rightarrow 1$ as $L \rightarrow \infty$.*

283 In the equation of Proposition 3, the terms κ_x and κ can both be normalized by a scalar
 284 and the resulting vector-matrix product is left unchanged. Specifically, if $\Theta_\infty^{(L)}$ is normalized
 285 such that its diagonal elements are all equal to 1, some immediate results follow from
 286 Propositions 1 and 2. These results are shown in Proposition 4 and Theorem 2.

288 **Definition 4** (Normalization of the $\Theta_\infty^{(L)}$ kernel). *For $x, x' \in S^{n_0-1}$, the normalized version
 289 of $\Theta_\infty^{(L)}$ is defined by*

$$291 \quad \bar{\Theta}_\infty^{(L)}(x, x') = \frac{n_0 2^{L-1} \Theta_\infty^{(L)}(x, x')}{L}.$$

293 **Definition 5.** *We define the function $h : [-1, 1] \rightarrow \mathbb{R}$ as*

$$295 \quad h(z) = \frac{z \arcsin(z)}{\pi} + \frac{\sqrt{1-z^2}}{\pi} + \frac{z}{2}.$$

297 Using the definitions above, we state the Proposition 4 and the Theorem 2. The proofs can
 298 be found in Appendix C.

300 **Proposition 4** (Alternative formulation of $\bar{\Theta}_\infty^{(L)}$). *The equality*

$$302 \quad \bar{\Theta}_\infty^{(L+1)}(x, x') = \frac{L}{L+1} h'(\rho^{(L)}(x, x')) \bar{\Theta}_\infty^{(L)}(x, x') + \frac{1}{L+1} h(\rho^{(L)}(x, x'))$$

304 *holds $\forall x, x' \in S^{n_0-1}$. Moreover, the values in the normalized kernel are all found in the
 305 interval $[0, 1]$.*

307 **Theorem 2** (Convergence of $\bar{\Theta}_\infty^{(L)}$). *For any $x, x' \in S^{n_0-1}$, the value $\bar{\Theta}_\infty^{(L)}(x, x')$ strictly
 308 increases to 1 as $L \rightarrow \infty$.*

310 The result above can be taken to be a major obstacle to the analysis of
 311 $\Theta_\infty^{(L)}(x^\top X^\top) \left(\Theta_\infty^{(L)}(XX^\top) \right)^{-1}$ since the positive determinant of $\Theta_\infty^{(L)}$ converges to 0. How-
 312 ever, Theorem 3 which is one of our key contributions, demonstrates that for a fixed x , the
 313 term $\Theta_\infty^{(L)}(x^\top X^\top) \left(\Theta_\infty^{(L)}(XX^\top) \right)^{-1}$ converges to some limit as L increases to infinity. The
 314 proof of this theorem requires a function defined in Definition 6 and whose key properties
 315 are provided as Proposition 5. The required background on rough differential equations is
 316 provided in Appendix D.

318 **Definition 6.** *We define the function ψ_d for $d \in \mathbb{R}^+$ as*

$$320 \quad \psi_d(z) = \begin{cases} \frac{1}{1 + \exp\left(\frac{-2z}{d(1-z^2)}\right)} & \text{if } z \in]-1, 1[\\ 1 & \text{if } z = 1 \\ 0 & \text{if } z = -1. \end{cases}$$

Proposition 5. *The function ψ_d has the following key properties on $[-1, 1]$:*

$$\psi_d(-1) = 0 \quad (1)$$

$$\psi_d(1) = 1 \quad (2)$$

$$\psi_d \in \mathcal{C}^\infty \quad (3)$$

$$\lim_{d \rightarrow 0^+} \frac{\frac{d^k}{dz^k} \psi_d(z)}{d^j} = 0 \quad \forall j, k \in \mathbb{N}_0. \quad (4)$$

Theorem 3 (Rough differential equation (RDE) solution). *In the compact regime, for each dataset X of size n (with entries x_i^\top) and $x \in S^{n_0-1}$, there exists a sequence of paths $v_{ij}^{(L)} : [0, 1] \rightarrow \mathbb{R}^n$ such that*

$$\lim_{L \rightarrow \infty} v_{ij}^{(L)}(t) = 0 \quad \forall t \in [0, 1]$$

and the rough path lift $\mathbf{v}^{(L)} : \Delta_{0,1} \rightarrow \mathbb{R}^{n \times n+1}$ of $v_{ij}^{(L)}$ with $p = 1$ **drives** the solution $\mathbf{u}^{(L)}$ of a differential equation

$$\frac{d}{dt} u_i^{(L)}(t) = 0 \quad \forall i \in \{1, \dots, n\},$$

and whose projection $(\mathbf{u}^{(L)})^1 = u^{(L)}$ onto 1-tensors satisfies the equality

$$u_i^{(L)}(1) = \bar{\Theta}_\infty^{(L)}(x^\top X)^\top \left(\bar{\Theta}_\infty^{(L)}(X^\top X) \right)^{-1}.$$

Here, $\Delta_{0,1}$ refers to the set $\{(s, t) : 0 \leq s \leq t\}$. Specifically,

$$\begin{aligned} \bar{\Theta}_\infty^{(L)}(x^\top X) \left(\bar{\Theta}_\infty^{(L)}(X^\top X) \right)^{-1} &< C(x) \mathbf{1}_n^\top \\ \left\| \left(\bar{\Theta}_\infty^{(L)}(X^\top X) \right)^{-1} \bar{\Theta}_\infty^{(L)}(X^\top x) \right\|_2 &\in \mathcal{O}(n) \end{aligned}$$

for L large enough. Moreover, when x is free and n is fixed, the function C is continuous and hence bounded on S^{n_0-1} .

Proof. We define the matrix $A_n^{(L+1)}(t)$ with

$$\begin{aligned} A_n^{(L+1)}(t) &= \bar{\Theta}_\infty^{(L)}(XX^\top) + \psi_{\mathcal{D}}(2t-1) \left(\bar{\Theta}_\infty^{(L+1)}(XX^\top) - \bar{\Theta}_\infty^{(L)}(XX^\top) \right) \\ \mathcal{D} &= \det \left(\bar{\Theta}_\infty^{(L+1)}(XX^\top) \right) \det \left(\bar{\Theta}_\infty^{(L)}(XX^\top) \right) \end{aligned}$$

for $t \in [0, 1]$ and dataset $X = \{x_i\}_{i=1}^n$ of size n . We also define $b_n^{(L+1)}(t)$ with

$$b_n^{(L+1)}(t) = \bar{\Theta}_\infty^{(L+1)}(x^\top X^\top).$$

From the system $A_n^{(L+1)}(t)u(t) = b_n^{(L+1)}(t)$, we take the derivative with respect to t and obtain the system

$$\left(\frac{d}{dt} A_n^{(L+1)}(t) \right) u(t) + A_n^{(L+1)}(t) \left(\frac{d}{dt} u(t) \right) = \frac{d}{dt} b_n^{(L+1)}(t).$$

Note that the solution $u(t)$ depends implicitly on n, L and x . This will be made obvious later in the proof, but it is hidden for cleaner notation. By Cramer's rule, the solution to the system is

$$u'(t)_i = \frac{\sum_j \det \left(A_n^{(L+1)}(t) \leftarrow_{i,j} Z_A \right)}{\det \left(A_n^{(L+1)}(t) \right)} + \frac{\det \left(A_n^{(L+1)}(t) \leftarrow_{i,1} Z_b \right)}{\det \left(A_n^{(L+1)}(t) \right)}, \quad (5)$$

where Z_A, Z_b are defined by

$$Z_A = - \left(\frac{d}{dt} A_n^{(L+1)}(t) \right) \text{diag}(u(t)), \quad Z_b = \frac{d}{dt} b_n^{(L+1)}(t) = \mathbf{0}_n,$$

where the boldface $\mathbf{0}_n$ denotes the vector of 0's of length n . By property (4) of $\psi_{\mathcal{D}}$, we obtain the sequence of inequalities

$$\begin{aligned}
& \frac{\det \left(A_n^{(L+1)}(t) \leftarrow_{i,j} \frac{d}{dt} A_n^{(L+1)}(t) \right)}{\det \left(A_n^{(L+1)}(t) \right)} && (v_{(i,j)}) \\
& \leq \frac{\det \left(A_n^{(L+1)}(t) \leftarrow_{i,j} \frac{d}{dt} A_n^{(L+1)}(t) \right)}{\det \left(\bar{\Theta}_{\infty}^{(L+1)}(XX^{\top}) \right)^{\psi_{\mathcal{D}}(2t-1)} \det \left(\bar{\Theta}_{\infty}^{(L)}(XX^{\top}) \right)^{1-\psi_{\mathcal{D}}(2t-1)}} \\
& \leq \frac{\det \left(A_n^{(L+1)}(t) \leftarrow_{i,j} \frac{d}{dt} A_n^{(L+1)}(t) \right)}{\det \left(\bar{\Theta}_{\infty}^{(L+1)}(XX^{\top}) \right) \det \left(\bar{\Theta}_{\infty}^{(L)}(XX^{\top}) \right)} \rightarrow 0 \quad \text{as } L \rightarrow \infty,
\end{aligned}$$

for L large enough. Note that we obtain the last inequality above through the fact that for L large enough, the strictly positive determinants are all smaller than 1. In addition, because, the function $\psi_{\mathcal{D}}$ is infinitely smooth, the terms $v_{(i,j)}$ are all of bounded total variation (see Definition 11 with $p = 1$ in the appendix). For the same reason and using (4), we have that the $v_{(i,j)}$ converge to 0 in the 1-variation metric. By Lyons Universal Limit theorem (Lyons, 1998) from rough path theory (see Definition 12 in the appendix), the solution $u^{(L+1)}(t)$ (where we make the dependence on $L + 1$ explicit) converges to the solution $u_{\infty}(t)$ that solves the system $u'_{\infty}(t) = \mathbf{0}_n$. Hence, $u_{\infty}(t)_i$ is a constant dependent on i and x . We have a limiting solution $u_{\infty}(t)$ that is bounded for each x . Because the Itô-Lyons map Φ (Definition 14 in appendix) is continuous and locally Lipschitz in any p -norm variation topology, and because the rough path lift of $v_{(i,j)}$ is continuous, the entire solution is bounded on the compact set S^{n_0-1} , i.e. there is a bound $C' < \infty$ such that $u_{\infty}(t) < C' \mathbf{1}_n$ for all x (note that $u_{\infty}(t)$ depends on x but not C'). \square

In summary, Theorem 3 provides a limiting solution for the expression $\bar{\Theta}_{\infty}^{(L)}(x^{\top} X^{\top}) \left(\bar{\Theta}_{\infty}^{(L)}(XX^{\top}) \right)^{-1}$ by solving systems of equations. The continuous solutions interpolate between solutions for different values of L . These systems are differentiated and formulated as rough differential equations that converge to a limiting RDE. The solution to this RDE at $t = 1$, i.e. the limiting expression, is dependent on x and non-trivial. Moreover, when evaluated at $x_i \in X$, $i \in \{1, \dots, n\}$, the limit is e_i , the i^{th} standard basis vector. While $\bar{\Theta}_{\infty}^{(L)}(XX^{\top})$ approaches a (constant) singular matrix, our proof shows that the limiting expression is well-defined. This distinguishes our approach from that of Xiao et al. (2020) (see Appendix D.3 in Xiao et al. (2020)), where $\bar{\Theta}_{\infty}^{(L)}(XX^{\top})$ is decoupled as a (constant) data-independent matrix and a data-dependent matrix whose limit is assumed to be invertible. Given that for any dataset X , Theorem 2 guarantees that $\bar{\Theta}_{\infty}^{(L)}(XX^{\top})$ converges to 1, the proof in Xiao et al. (2020) would not apply.

An immediate consequence of this result is that if the depth $L \in o(\min_{1 \leq l < L-1} n_l)$ and the width $(\min_{1 \leq l \leq L-1} n_l)$ both go to infinity (i.e. the ratio of depth to width going to 0), the kernel of the output f_{∞} of the neural network reaches a limiting expression. This limiting expression characterizes the effect of depth on infinitely wide fully-connected ReLU networks whose inputs lie on the sphere S^{n_0-1} . For ReLU networks, it is possible to easily extend this result to the non-compact regime (i.e. general domain \mathbb{R}^{n_0}). By Proposition 2 there is a closed-form to Θ_{∞} for general data points in \mathbb{R}^{n_0} . In the statement of the proposition, the canonical projection on the sphere is provided, but a similar result is obtained for a stereographic projection.

6 EXPERIMENTS AND THEORETICAL IMPLICATIONS

In the proof of Theorem 3 from the previous section, we can identify the key properties used to derive the results, in order to distill the essence of the type of kernels that lead to similar limiting behaviour. We summarize these properties for data on S^{n_0-1} .

432 **Arbitrary sequence of kernels $\kappa^{(L)}$ satisfying the requirements of the theorem**

- 433
- 434 • $\kappa^{(L)}(x, x) \geq \kappa^{(L)}(x_1, x_2)$ for any $x, x_1, x_2 \in S^{n_0-1}$ and all $L \in \mathbb{N}$.
 - 435 • There is some $\hat{L} \in \mathbb{N}$ such that $\kappa^{(L)}(XX^\top)$ is positive definite for any $X =$
 - 436 $\{x_i \mid x_i \in S^{n_0-1}, i = 1, \dots, n\}$ of size n and $L \geq \hat{L}$.
 - 437 • $\lim_{L \rightarrow \infty} \det(\bar{\kappa}^{(L)}(XX^\top)) = 0$ for data in S^{n_0-1} .
- 438

439

440 By inspection of the definition of $\rho^{(L)}$, it can be observed that it satisfies the criteria of the list

441 above. Another example is given by the sequence $\eta^{(L)}$ of kernels that are defined recursively

442 by $\eta^{(L+1)}(x, x') = h(\kappa^{(L)}(x, x'))$ and $\eta^{(1)}(x, x') = x^\top x'$, where $h(z) = (1 + e^{-z})^{-2}$ (see

443 Proposition [7](#) in the appendix).

444

445 In order to better understand the theoretical insights from the previous section, we empirically

446 evaluate the convergence rates of $\bar{\Theta}_\infty^{(L)}$, $\rho^{(L)}$ and η as L increases. We illustrate this convergent

447 behavior in figure [1](#), where we generate a dataset X and a point x from the uniform

448 distribution ($n_0 = 128$) and we canonically project them to the sphere. We then plot the

449 evolution of the values for depths $L = 1, \dots, 30$. **Note that this depth limit is sufficient to**

450 **show convergence.** Each curve in the plots corresponds to a different pair of inputs (either

451 from X or between x and X ; e.g. $\bar{\Theta}_\infty^{(L)}(x_i, x_j)$). It is immediate at first glance that both $\rho^{(L)}$

452 and $\eta^{(L)}$ converge to a fixed value rather quickly as the depth increases. In contrast, from the

453 plot of $\bar{\Theta}_\infty^{(L)}(XX^\top)$, while it is seemingly the case that off-diagonal values converge to some

454 value strictly smaller than 1, Theorem [2](#) demonstrates that they converge to 1. **In addition**

455 **to the synthetic dataset X , we perform the same experiment on the MNIST dataset** ([LeCun](#)

456 [et al., 2010](#)), whose tensors are converted to vectors that are normalized to lie on the sphere.

457 **We report the results in figure [3](#) in Appendix [F](#). In both datasets, the convergence rate**

458 **is sublinear for $\bar{\Theta}_\infty^{(L)}(XX^\top)$ and it is possible to observe this directly in the proof of the**

459 **theorem: K is taken to be much larger than L , and given an approximation threshold of**

460 **$0 < \delta \ll 1$, the exponential approximation to $(1 - \delta)^{K+1}$ requires that $K\delta \gg 0$, i.e. K**

461 **is much larger than $\frac{1}{\delta}$. The convergence rate to 1 can in fact be shown to be logarithmic.**

462 **Nevertheless, by inspection of the proof of Theorem [3](#), we can see that $(v_{(i,j)})$ converges to 0**

463 **exponentially faster than $\det(\bar{\Theta}_\infty^{(L)}(XX^\top))$. This serves to show that the convergence to**

464 **the limiting solution is fast, provided the determinant is small. We numerically evaluate this**

465 **determinant by computing it in figure [2](#) for MNIST in Appendix [F](#). We hypothesize that**

466 **small determinants indicate fast convergence to the limiting solution. This would suggest**

467 **that depths L that are not very large are sufficient for a good approximation to the limiting**

468 **solution. While we do not explore any other kernels experimentally, we refer the reader to**

469 **the list of criteria in this section to derive any other candidate to explore its convergence**

470 **properties.**

471 Note that [Bietti & Bach \(2021\)](#) and [Li et al. \(2024\)](#) tell us that the representation power of

472 $\Theta_\infty^{(L)}$ does not change as $L \rightarrow \infty$. However, if we apply our limiting result to the mean-field

473 regime of [Chizat & Bach \(2018\)](#), we find that each particle approaches the deterministic

474 limit by inspection of Proposition [3](#) and Theorem [3](#). It is therefore possible to analyze the

475 many-particle limit of very wide and deep fully-connected neural networks since these are

476 well approximated by f_τ for a proper stopping time τ ([Li et al., 2024](#)). In addition, the proof

477 technique of Theorem [3](#) can be adapted to other kernels that arise from other architectures

478 such as CNNs.

479

480 **7 CONCLUSION**

481

482 In this article, we provide a detailed analysis of behaviour of the deterministic kernel

483 $\Theta_\infty^{(L)}$ as $L \rightarrow \infty$. We observe that under the conditions of [Jacot et al. \(2018a\)](#) and with

484 $L \in o(\min_{l=1, \dots, L-1} n_l)$, a fully-connected ReLU neural network approaches a limiting

485 solution for any x given a fixed dataset X . **The studied kernel exhibits behaviour consistent**

with the ordered phase. In contrast to [Xiao et al. \(2020\)](#), we do not assume that the limiting

486
487
488
489
490
491
492
493
494
495
496
497
498
499
500
501
502
503
504
505
506
507
508
509
510
511
512
513
514
515
516
517
518
519
520
521
522
523
524
525
526
527
528
529
530
531
532
533
534
535
536
537
538
539

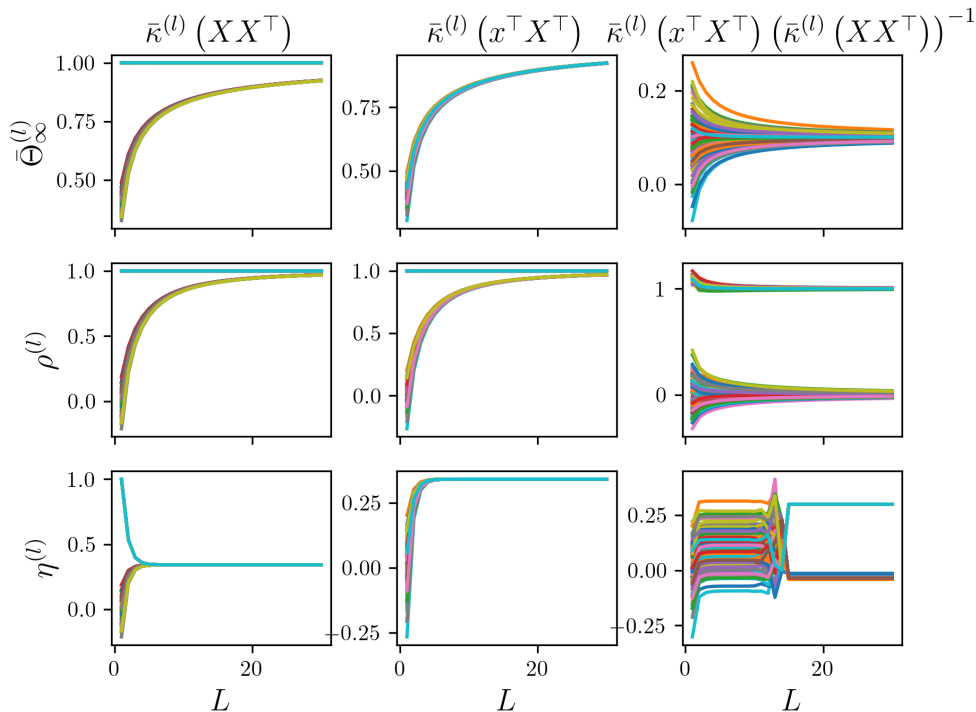


Figure 1: Convergence rate of κ on X and point x . We model 3 different expressions dependent on an arbitrary κ in each column. The particular choice of κ is given by each row (see label on the left).

kernel can be written as the sum of a constant and a non-singular matrix. We generalize the existence of a limiting solution for $\kappa_x \kappa^{-1}$ to include the singular case. While our results are for data in S^{n_0-1} , we can extend this result to the general domain as long as there is no colinearity, or by taking the stereographic projection in a space with one additional dimension. On the one hand, we have shown the convergence rates of a non-exhaustive list of kernels as depth L increases. For the limiting kernels $\kappa^{(L)} = \Theta_\infty^{(L)}$, we have observed that the convergence is extremely slow and would require very large L before reaching the limit. On the other hand, small depths L are required to approximate the limit of $\kappa_x \kappa^{-1}$. Specifically, we demonstrate empirically that, while convergence for the limiting kernel is sublinear, the convergence for the limiting kernel is experimentally fast. We hypothesize that this will be the case in many scenarios. Studying the settings in which this is true is left as a future research direction. Finally, we provided a list of key properties that were necessary to obtain our results to generalize to other kernels.

We believe that our work can help researchers to better understand the role of depth in the deterministic limiting kernels of overparameterized neural networks. Future research should envisage to better understand the behaviour of kernels that arise in the context of other architectures such as CNNs and architectures with skip connections. As mentioned, the setting of Hanin & Nica (2020) is outside the purview of our analysis as the stochasticity of the NTK becomes highly relevant when $L \gg \max_{l=1, \dots, L-1} n_l$. Nevertheless, by using the analytical tools of rough differential equations, we raise the hypothesis that there might exist a “pointwise” limit to the NTK when $L \rightarrow \infty$, where it is implied that the convergence is with respect to each sample path.

540
541
542
543
544
545
546
547
548
549
550
551
552
553
554
555
556
557
558
559
560
561
562
563
564
565
566
567
568
569
570
571
572
573
574
575
576
577
578
579
580
581
582
583
584
585
586
587
588
589
590
591
592
593

REFERENCES

- Zeyuan Allen-Zhu, Yuanzhi Li, and Zhao Song. A convergence theory for deep learning via over-parameterization. In *International conference on machine learning*, pp. 242–252. PMLR, 2019.
- Sanjeev Arora, Simon Du, Wei Hu, Zhiyuan Li, and Ruosong Wang. Fine-grained analysis of optimization and generalization for overparameterized two-layer neural networks. In *International conference on machine learning*, pp. 322–332. PMLR, 2019a.
- Sanjeev Arora, Simon S Du, Wei Hu, Zhiyuan Li, Russ R Salakhutdinov, and Ruosong Wang. On exact computation with an infinitely wide neural net. *Advances in neural information processing systems*, 32, 2019b.
- Mikhail Belkin. Fit without fear: remarkable mathematical phenomena of deep learning through the prism of interpolation. *Acta Numerica*, 30:203–248, 2021.
- Alberto Bietti and Francis Bach. Deep equals shallow for relu networks in kernel regimes. In *ICLR 2021-International Conference on Learning Representations*, pp. 1–22, 2021.
- Lenaic Chizat and Francis Bach. On the global convergence of gradient descent for over-parameterized models using optimal transport. *Advances in neural information processing systems*, 31, 2018.
- Youngmin Cho and Lawrence Saul. Kernel methods for deep learning. In Y. Bengio, D. Schuurmans, J. Lafferty, C. Williams, and A. Culotta (eds.), *Advances in Neural Information Processing Systems*, volume 22. Curran Associates, Inc., 2009. URL https://proceedings.neurips.cc/paper_files/paper/2009/file/5751ec3e9a4feab575962e78e006250d-Paper.pdf
- Tilman Gneiting. Strictly and non-strictly positive definite functions on spheres. *Bernoulli*, 19(4):1327 – 1349, 2013. doi: 10.3150/12-BEJSP06. URL <https://doi.org/10.3150/12-BEJSP06>
- Boris Hanin and Mihai Nica. Finite depth and width corrections to the neural tangent kernel. In *8th International Conference on Learning Representations, ICLR 2020*, 2020.
- Arthur Jacot, Franck Gabriel, and Clément Hongler. Neural tangent kernel: Convergence and generalization in neural networks. *Advances in neural information processing systems*, 31, 2018a.
- Arthur Jacot, Franck Gabriel, and Clément Hongler. Neural tangent kernel: Convergence and generalization in neural networks. *arXiv preprint arXiv:1806.07572*, 2018b. URL <https://arxiv.org/abs/1806.07572>
- Yann LeCun, Léon Bottou, Yoshua Bengio, and Patrick Haffner. Gradient-based learning applied to document recognition. *Proceedings of the IEEE*, 86(11):2278–2324, 1998.
- Yann LeCun, Corinna Cortes, and CJ Burges. Mnist handwritten digit database. *ATT Labs [Online]*. Available: <http://yann.lecun.com/exdb/mnist/>, 2, 2010.
- Jaehoon Lee, Lechao Xiao, Samuel Schoenholz, Yasaman Bahri, Roman Novak, Jascha Sohl-Dickstein, and Jeffrey Pennington. Wide neural networks of any depth evolve as linear models under gradient descent. *Advances in neural information processing systems*, 32, 2019.
- Jaehoon Lee, Samuel Schoenholz, Jeffrey Pennington, Ben Adlam, Lechao Xiao, Roman Novak, and Jascha Sohl-Dickstein. Finite versus infinite neural networks: an empirical study. *Advances in Neural Information Processing Systems*, 33:15156–15172, 2020.
- Jongmin Lee, Joo Young Choi, Ernest K Ryu, and Albert No. Neural tangent kernel analysis of deep narrow neural networks. In *International Conference on Machine Learning*, pp. 12282–12351. PMLR, 2022.

594 Yicheng Li, Zixiong Yu, Guhan Chen, and Qian Lin. On the eigenvalue decay rates of a
595 class of neural-network related kernel functions defined on general domains. *Journal of*
596 *Machine Learning Research*, 25(82):1–47, 2024.
597

598 Chaoyue Liu, Libin Zhu, and Misha Belkin. On the linearity of large non-linear models:
599 when and why the tangent kernel is constant. *Advances in Neural Information Processing*
600 *Systems*, 33:15954–15964, 2020.

601 Chaoyue Liu, Libin Zhu, and Mikhail Belkin. Loss landscapes and optimization in over-
602 parameterized non-linear systems and neural networks. *Applied and Computational*
603 *Harmonic Analysis*, 59:85–116, 2022.

604 Terry J Lyons. Differential equations driven by rough signals. *Revista Matemática Iberoamer-*
605 *icana*, 14(2):215–310, 1998.
606

607 Michael Murray, Hui Jin, Benjamin Bowman, and Guido Montufar. Characterizing the
608 spectrum of the ntk via a power series expansion. In *International Conference on Learning*
609 *Representations*, 2023.

610 Quynh Nguyen, Marco Mondelli, and Guido F Montufar. Tight bounds on the smallest
611 eigenvalue of the neural tangent kernel for deep relu networks. In *International Conference*
612 *on Machine Learning*, pp. 8119–8129. PMLR, 2021.

613 Maria Seleznova and Gitta Kutyniok. Analyzing finite neural networks: Can we trust neural
614 tangent kernel theory? In *Mathematical and Scientific Machine Learning (MSML)*, 2022.
615

616 David Silver, Thomas Hubert, Julian Schrittwieser, Ioannis Antonoglou, Matthew Lai, Arthur
617 Guez, Marc Lanctot, Laurent Sifre, Dhharshan Kumaran, Thore Graepel, Timothy Lillicrap,
618 Karen Simonyan, and Demis Hassabis. A general reinforcement learning algorithm that
619 masters chess, shogi, and go through self-play. *Science*, 362(6419):1140–1144, 2018. doi:
620 10.1126/science.aar6404. URL [https://www.science.org/doi/abs/10.1126/science](https://www.science.org/doi/abs/10.1126/science.aar6404)
621 [aar6404](https://www.science.org/doi/abs/10.1126/science.aar6404).

622 Russell Tsuchida, Fred Roosta, and Marcus Gallagher. Invariance of weight distributions in
623 rectified mlps. In *International Conference on Machine Learning*, pp. 4995–5004. PMLR,
624 2018.
625

626 Ashish Vaswani, Noam Shazeer, Niki Parmar, Jakob Uszkoreit, Llion Jones, Aidan N Gomez,
627 Łukasz Kaiser, and Illia Polosukhin. Attention is all you need. *Advances in neural*
628 *information processing systems*, 30, 2017.

629 Lechao Xiao, Jeffrey Pennington, and Samuel Schoenholz. Disentangling trainability and
630 generalization in deep neural networks. In *Proceedings of the 37th International Conference*
631 *on Machine Learning (ICML)*, 2020.
632
633
634
635
636
637
638
639
640
641
642
643
644
645
646
647